

VISCOELASTIC MODULATION OF SOLITARY PRESSURE PULSES IN NONLINEAR FLUID-FILLED DISTENSIBLE TUBES

By GORDON E. SWATERS

(*Applied Mathematics Institute, Department of Mathematics, University of Alberta, Edmonton, Alberta, Canada T6G 2G1*)

and RONALD P. SAWATZKY

(*Department of Mathematics, University of Arizona, Tucson, Arizona 85721, USA*)

[Received 15 April 1988. Revise 20 August 1988]

SUMMARY

The propagation of small-but-finite-amplitude weakly-dispersive pressure pulses in a viscoelastic fluid-filled tube is shown to be governed by a Korteweg–de Vries–Burgers (KdVB) equation. We present a direct singular perturbation theory to describe the viscoelastic modulation of solitary pressure pulses for small retardation times. The main pulse evolves so as to satisfy a leading-order energy balance resulting in an algebraic decay in the amplitude and translation speed of the solution. Higher-order energy balances imply a monotonically increasing positive phase shift.

A complete description of the first-order perturbation pressure is given. A pressure shelf of finite extent is continuously excited in the lee of the propagating pulse. The shelf extends from the current location of the solitary pressure pulse to the Korteweg–Moens phase position. The transition of the pressure shelf back to a zero background state at the Korteweg–Moens phase position is accomplished through a series of viscoelastically modified spatially-decaying high-wavenumber oscillations. Ahead of the main pulse a uniformly valid perturbation pressure field is obtained via a combination WKB–power-series and similarity-solution procedure.

1. Introduction

MANY of the properties of propagating pressure pulses in fluid-filled distensible tubes can be described by a non-dispersive hyperbolic low-wavenumber linear theory (1) in which the physical mechanism responsible for the wave propagation is essentially a balance between the hoop stress in the tube wall and the transmural pressure drop (2, 3); that is, the so-called tube law. Cowley (4, 5) demonstrated how the tube law could be systematically derived from nonlinear cylindrical membrane theory (6) in the limit of zero axial wavenumber and infinitesimal pulse amplitudes.

However, while the propagation *velocity* of the pressure pulse is well approximated by the results of the above linear theory, there are several important aspects of propagating pressure pulses in fluid-filled elastic tubes which the above theory cannot describe. For example, the pulse attenuation

and broadening that has been observed in experimental studies cannot be reproduced (7 to 12). In order to correctly describe these properties additional physics is required such as wavenumber dispersion, tube-wall viscoelasticity and fluid viscosity (see (13)). As well, phenomena such as elastic jump formation and propagation, the onset of a collapse (14), or wave-wave interactions will require a nonlinear theory; for example, (15, 16, 4, 5, 17).

It is possible to crudely estimate the relative importance of all these processes from the experimental data cited above. In what follows we are implicitly assuming that the 'tube-law' balance is dynamically dominant. It can be shown (see section 2) that the effects of wavenumber dispersion make a cumulative contribution to the evolution of the pulse as important as the tube-law balance when the pulse has travelled through a distance of approximately $O[(L/a_0)^2]$ tube radii, where L is a typical horizontal length scale of the pulse and a_0 is the undisturbed tube radius. Based on the data presented in (7 to 12) we compute $(L/a_0)^2 \approx 50$. On the other hand, it is easy to show that nonlinearity makes a cumulative contribution to the pulse evolution as important as the tube-law balance after the pulse has travelled through a distance of $O[\rho c_0^2/\Delta p^*]$ tube radii, where ρ is the fluid density, c_0 is the Korteweg-Moens phase speed and Δp^* is a measure of the pulse pressure relative to the ambient pressure (say at time of initiation). From the data we find that $\rho c_0^2/\Delta p^* \approx 10$ to 30. Finally, the effects of wall viscoelasticity will make a cumulative contribution to the evolution of the pulse as important as the tube-law balance after the pulse has travelled through a distance of $O[T_0/T_c]$ tube radii, where T_0 and T_c are, respectively, a time scale associated with the pressure-pulse propagation and a viscoelastic characteristic time. Again, based on experimental data we find that $T_0/T_c \approx 80$ to 100. Thus, as a rough estimate, the experimental data suggest that the effects of nonlinearity, dispersion and viscoelasticity are relatively weak but make a cumulative contribution as important as the tube law to the evolution of the pressure pulse after the pulse has travelled a distance of several tens of tube radii.

Cowley (5, 18) showed that small-amplitude weakly-dispersive turbulent elastic jumps, propagating in a fluid-filled hyperelastic tube can radiate energy through a cnoidal wavetrain described by a Korteweg-de Vries equation. In the case of laminar elastic jumps Cowley showed that they were governed by a perturbed Korteweg-de Vries equation with a Rayleigh damping term. The principal objective of this paper is to present a multiple-scales singular-perturbation theory describing the propagation of small-but-finite-amplitude weakly-dispersive coherent pressure pulses in a nonlinear fluid-filled Kelvin-Voigt viscoelastic tube with a small characteristic time. We shall show that such pulses are governed by a Korteweg-de Vries-Burgers equation.

Previously, Ravinchan and Prasad (19) had shown for a Maxwell

viscoelastic tube-wall model that long small-amplitude pressure pulses were described by a Korteweg–de Vries–Burgers equation. However, no analysis of any kind was presented detailing the propagation characteristics of solitary or periodic pressure pulses. Here, we shall give a complete asymptotic description of the evolution of a solitary pressure pulse and associated perturbation pressure field, assuming a relatively small non-dimensional retardation time for the tube wall. Our procedures are modifications and extensions of the asymptotic and inverse-scattering theory developed to study the Rayleigh-perturbed Korteweg–de Vries equation (20 to 26).

We may briefly summarize our principal results as follows. The main pulse evolves adiabatically so as to satisfy a leading-order energy balance (21, 23, 25) which will result in an algebraic decay in the soliton amplitude and translation speed relative to the Korteweg–Moens phase speed. (The soliton always travels faster than the Korteweg–Moens phase speed due to the action of nonlinearity.) The above decay rate is in sharp contrast to the exponential decay obtained for Rayleigh damping and reflects the ‘local’ structure of the viscoelastic differential operator (that is, proportional to the curvature rather than amplitude) in the KdV equation. Eventually the amplitude of the soliton decreases to the point where further evolution is essentially a balance between dispersive and dissipative processes alone. Higher-order energy balances for the dissipating solitary pulse will be shown to result in a monotonically increasing positive phase shift.

The structure of the pressure field at a given station once the pulse has passed is complex (see Fig. 1). The perturbation pressure field immediately behind the main pulse can be obtained via an adiabatic comoving ansatz. However, the adiabatic perturbation pressure field is shown to be exponentially non-uniform in space and time behind the main pulse. This non-uniformity corresponds to the existence of a pressure shelf of finite extent which trails behind the main pulse. The shelf represents a small-amplitude (on the order of the non-dimensional retardation time) dilation of the tube. The dilation extends from the decaying main pulse to the current position associated with a hypothetical Korteweg–Moens pulse (24, 26). Beginning at the Korteweg–Moens phase position, the shelf undergoes a series of viscoelastically modified high-wavenumber oscillations (that is, a dissipative and dispersive wavetrain) in the transition to a zero-amplitude background state.

A complete asymptotic description of the perturbation pressure field ahead of the main pulse is also given. We shall show that the comoving perturbation pressure field is algebraically non-uniform ahead of the main pulse. Following the asymptotic procedures of Johnson (20) and Kodama and Ablowitz (25) we are able to obtain exact asymptotic solutions for the perturbation pressure field ahead of the main pulse. In the near-field a WKB solution can be obtained in which the phase and amplitude are

obtained in the form of a power-series in a stretched Kortweg–Moens phase variable. In the far field the power-series solution is no longer valid and a similarity solution for the WKB phase and amplitude is required. We are able to find exact similarity solutions for this region.

The plan of the paper is as follows. In section 2 the problem is formulated and the Korteweg–de Vries–Burgers (KdVB) equation for the pulse pressure is derived. In section 3 we present an asymptotic solution to KdVB for small relaxation times. In section 4 we describe the asymptotic solution and in section 5 we make some concluding remarks.

2. Problem formulation and derivation of the Korteweg–de Vries–Burgers equation

We begin by assuming that the inviscid, homogeneous fluid within the tube is perturbed by an axisymmetric disturbance. The dynamics of the tube wall are described by a Kelvin–Voigt viscoelastic cylindrical axially-tethered shell theory. The Kelvin–Voigt viscoelastic tube-wall model adopted here is essentially that derived by Moodie *et al.* (10, 27) and successfully tested experimentally (11, 12). Our derivation of the KdVB equation will be relatively brief since the asymptotic balances are well known and can be found in, for example, (5, 19).

The nonlinear *dimensional* equations for the fluid can be written in the form

$$(r^*u^*)_{x^*} + (r^*v^*)_{r^*} = 0, \tag{2.1}$$

$$u_{t^*}^* + u^*u_{x^*}^* + v^*u_{r^*}^* + \frac{1}{\rho}p_{x^*}^* = 0, \tag{2.2}$$

$$v_{t^*}^* + u^*v_{x^*}^* + v^*v_{r^*}^* + \frac{1}{\rho}p_{r^*}^* = 0, \tag{2.3}$$

where x^*, r^* are the longitudinal and radial coordinates respectively, u^*, v^* are the associated velocity components, and p^* and ρ are the pressure and density of the fluid, respectively. The axial- and radial-momentum equations are given by (2.2) and (2.3), respectively, and (2.1) expresses mass conservation.

The appropriate *boundary* conditions on (2.1), (2.2) and (2.3) are

$$v^* = a_{t^*}^* + u^*a_{x^*}^* \quad \text{on } r^* = a^*, \tag{2.4}$$

$$p^* = \rho_w h a_{t^*}^* - \dot{\rho}_w h^3 a_{x^*}^* a_{r^*}^* / 12 + 4G_e(1 + T_c \partial_{t^*}) (h a^* / a_0^2 + h^3 a_{x^*}^* a_{x^*}^* / 12) + \text{h.o.t.} \quad \text{on } r^* = a^*, \tag{2.5}$$

where ρ_w, h, a_0, G_e and T_c are the wall density, wall thickness, undeformed

initial radial position of the shell wall, the equilibrium elastic shear modulus, and dimensional retardation time of the viscoelastic tube wall, respectively. The time-dependent position of the tube wall is denoted by $a^*(x^*, t^*)$.

The pressure-boundary condition (2.5) (that is, the viscoelastic shell-wall model) retains several features which are important in a dynamically active viscoelastic shell. Physically, the terms on the right-hand side of (2.5) correspond to radial inertia, rotatory inertia, flexural rigidity and circumferential stiffness, respectively, from left to right. Implicit in (2.5) is the assumption that there is no applied *external* pressure. The higher-order terms (h.o.t.) not explicitly included in (2.5) are primarily the nonlinear convective accelerations and nonlinear corrections to the tube-wall curvature. It is possible to show that these terms are at least two orders of magnitude smaller than the leading terms in (2.5) and consequently will play no role in our analysis. The viscoelastic shell-wall model (2.5) differs from the model assumed by Ravinchan and Prasad (19) in several respects. Besides the choice of the Kelvin–Voigt viscoelastic model (which we shall comment on momentarily), the model (2.5) retains terms corresponding to the rotatory inertia, flexural rigidity and circumferential stiffness of the tube wall. These terms do not appear in (19). With respect to the choice of the viscoelastic model, it is well known that for the relatively low wavenumber and frequency motions examined here, the Kelvin–Voigt model is the most appropriate choice for a material in which the response to a stress change after a sufficiently long time is elastic rather than viscous (28) as opposed to the Maxwell model in (19). Perhaps of equal importance to the above remarks is the fact that (2.5) has been used to model many aspects of pulse propagation in viscoelastic tubes (11, 12) and therefore an analysis of its predictions in the weakly-nonlinear and weakly-dispersive limit is of interest.

Note that in (2.2) and (2.3) the effects of fluid viscosity have been neglected. Comparisons between theoretical calculations and observed pressure pulses in, for example, latex tubes have demonstrated that the amplitude- and frequency-dependent dissipation is mainly the result of viscoelastic effects in the tube wall rather than fluid viscosity (12, 29).

Further analysis is facilitated by defining the non-dimensional (unasterisked) variables:

$$\left. \begin{aligned} t^* &= (L/c_0)t, & x^* &= Lx, & r^* &= a_0r, \\ p^* &= \rho c_0^2(2 + \varepsilon p), & u^* &= \varepsilon c_0 u, \\ v^* &= \varepsilon^{\frac{1}{2}} c_0 v, & a^* &= a_0(1 + \varepsilon \varphi), \end{aligned} \right\} \quad (2.6)$$

where $c_0^2 \equiv 2G_e h(\rho a_0)^{-1}$ is the squared Korteweg–Moens phase speed for linear non-dispersive pressure pulses in fluid-filled elastic tubes (13), and $\varepsilon \equiv (a_0/L)^2$. In what follows we assume that $0 < \varepsilon \ll 1$. This limit will

correspond to the propagation of small-but-finite-amplitude weakly-dispersive and dissipative pressure pulses.

Substitution of (2.6) into the governing equations shows that to leading order in ϵ the equations are hyperbolic with characteristics given by $x \pm t$, and that the nonlinear modulation, dispersion and viscoelastic effects occur on a space-time scale of $O(\epsilon^{-1})$. In what follows we focus attention on the rightward-travelling (that is, $x > 0$) pulse. Consequently, we introduce the non-dimensional *fast Korteweg-Moens* phase variable and *slow* space variable

$$\theta = x - t, \quad X = \epsilon x, \tag{2.7}$$

respectively. We work with a slow space rather than time variable because many experimental configurations correspond to signalling as opposed to initial-value problems.

The resulting non-dimensional problem can be put into the form

$$(rp_r)_r + \epsilon rp_{\theta\theta} + 2\epsilon^2 rp_{\theta X} = -\epsilon^2 r[uv_\theta + vu_r]_\theta - \epsilon^2 [r(uv_\theta + vv_r)]_r + O(\epsilon^3), \tag{2.8}$$

$$u_\theta = p_\theta + \epsilon p_X + \epsilon uu_\theta + \epsilon vv_r + O(\epsilon^2), \tag{2.9}$$

$$\epsilon v_\theta = p_r + \epsilon^2 uv_\theta + \epsilon^2 vv_r + O(\epsilon^3), \tag{2.10}$$

together with the boundary conditions (expanded about $\epsilon = 0$)

$$v = -\varphi_\theta - \epsilon \varphi v_r + \epsilon u \varphi_\theta + O(\epsilon^2), \tag{2.11}$$

$$p = 2\varphi - \epsilon \varphi p_r - 2\epsilon \hat{\mu} \varphi_\theta + \epsilon \delta \varphi_{\theta\theta} + O(\epsilon^2), \tag{2.12}$$

evaluated on $r = 1$. The parameters $\hat{\mu} \equiv T_c c_0 (\epsilon L)^{-1}$, $\delta \equiv h \rho_w (a_0 \rho)^{-1}$ are the non-dimensional viscoelastic characteristic time and radial-inertia coefficients, respectively. It will be formally assumed that both parameters are $O(1)$, although the smallness of $\hat{\mu}$ will be eventually demanded for further analytical progress; that is, $0 < \epsilon \ll \hat{\mu} \ll 1$.

The equations (2.8) to (2.12) possess a straightforward asymptotic solution in the form

$$(u, v, p)(\theta, r; X) = \sum_{n=0}^{\infty} \epsilon^n (u, v, p)^{(n)}(\theta, r; X), \tag{2.13a}$$

$$\varphi(\theta, X) = \sum_{n=0}^{\infty} \epsilon^n \varphi^{(n)}(\theta; X). \tag{2.13b}$$

The $O(1)$ -problem is simply

$$(rp_r^{(0)})_r = 0, \tag{2.14}$$

$$u_\theta^{(0)} = p_\theta^{(0)}, \tag{2.15}$$

$$p_r^{(0)} = 0, \tag{2.16}$$

$$v^{(0)} = -\varphi_{\theta}^{(0)} \quad \text{on } r = 1, \tag{2.17}$$

$$p^{(0)} = 2\varphi^{(0)} \quad \text{on } r = 1. \tag{2.18}$$

To this order the problem does not have a unique solution since (2.16) makes (2.14) vacuous.

Assuming a localized coherent solution for $p^{(0)}$ (that is, $p^{(0)}$ has compact support in θ), the $O(1)$ -problem possesses a general solution in the form

$$p^{(0)} = F(\theta; X), \tag{2.19}$$

$$u_{\theta}^{(0)} = F(\theta; X), \tag{2.20}$$

$$\varphi^{(0)} = \frac{1}{2}F(\theta; X), \tag{2.21}$$

$$v^{(0)} = -\frac{1}{2}F_{\theta}(\theta; X) \quad \text{on } r = 1, \tag{2.22}$$

where $F(\theta; X)$ is undetermined at this stage. We shall show that $F(\theta; X)$ satisfies a KdVB equation.

The $O(\epsilon)$ -problem can be put into the form

$$(rp_r^{(1)})_r = -rF_{\theta\theta}, \tag{2.23}$$

$$u_{\theta}^{(1)} = p_{\theta}^{(1)} + F_X + FF_{\theta}, \tag{2.24}$$

$$v_{\theta}^{(0)} = p_r^{(1)}, \tag{2.25}$$

$$v^{(1)} = -\varphi_{\theta}^{(1)} - \frac{1}{2}Fv_r^{(0)} + \frac{1}{2}FF_{\theta} \quad \text{on } r = 1, \tag{2.26}$$

$$p^{(1)} = 2\varphi^{(1)} - \hat{\mu}F_{\theta} + \delta F_{\theta\theta} \quad \text{on } r = 1. \tag{2.27}$$

It follows from (2.23) and (2.25) that

$$p^{(1)} = -\frac{1}{4}r^2F_{\theta\theta}, \tag{2.28}$$

$$v^{(0)} = -\frac{1}{2}rF_{\theta}. \tag{2.29}$$

Note that (2.29) is consistent with (2.22).

To close the problem and determine the evolution of $F(\theta; X)$ we need only examine the $O(\epsilon^2)$ -continuity and radial-momentum equations given by, respectively,

$$(rp_r^{(2)})_r = 2rF_{\theta X} + \frac{1}{4}r^3F_{\theta\theta\theta\theta} - \frac{3}{2}rF_{\theta}F_{\theta}, \tag{2.30}$$

$$v_{\theta}^{(1)} = p_r^{(2)} - \frac{1}{2}rFF_{\theta\theta} + \frac{1}{4}rF_{\theta}F_{\theta}. \tag{2.31}$$

The pressure $p^{(2)}$ can be eliminated between these two expressions to yield

$$v^{(1)}(r, \theta; X) = -rF_X + \frac{1}{16}r^3F_{\theta\theta\theta\theta} - \frac{1}{2}rFF_{\theta}. \tag{2.32}$$

However, (2.26) to (2.29) and (2.32) are consistent if and only if

$$q_{\tau} - 6qq_{\theta} + q_{\theta\theta\theta} = \mu q_{\theta\theta}, \tag{2.33a}$$

where

$$\left. \begin{aligned} q(\theta; \tau) &= -10F(\theta; X)[3(1 + 8\delta)]^{-1}, \\ \tau &= \frac{1}{16}X(1 + 8\delta), \\ \mu &= 8(1 + 8\delta)\hat{\mu}. \end{aligned} \right\} \quad (2.33b)$$

Equation (2.33) is a Korteweg–de Vries–Burgers equation. The KdVB equation has been proposed as a model for many physical problems when nonlinear, dispersive and dissipative processes are all of the same (small) order of magnitude (30 to 35); for a brief review see Craik (36). Kawahara (33) has argued that it is possible to interpret the *dispersive* term in (2.33) as an effective impedance to the nonlinear mode–mode coupling which ultimately can lead to higher-amplitude equilibria in the form of a row of soliton-like pulses. For strong dissipation and weak dispersion, the steadily-travelling bounded solutions to (2.33) resemble the Burgers shock wave (34).

The qualitative behaviour of the steadily-travelling bounded solutions to (2.33) can be summarized as follows (Jeffrey and Kakutani (37)). If $\mu > \mu_c \equiv 2[c^2 + \beta]^{\frac{1}{2}} > 0$, where c is the propagation velocity and β is an amplitude parameter (which depends implicitly on c), then the solutions resemble the Burgers shock wave with an accompanying wave train. If $0 < \mu < \mu_c$, the periodic solutions resemble cnoidal waves. For $0 < \mu \ll \mu_c$, the solutions will resemble damped cnoidal or solitary waves.

Kawahara and Toh (38) and Malomed (39) have examined the evolution of the non-soliton and periodic cnoidal-wave solutions to (2.33) subject to weak dissipation. For applications to coherent pulse propagation in viscoelastic tubes, it is of interest to develop a theory which describes the modulation of solitary pressure pulses for the limit $0 < \mu \ll \mu_c$. In a subsequent paper we shall present the results of a numerical study on the evolution of pressure pulses for more arbitrary compact initial data and a wide range of viscoelastic characteristic times.

3. Asymptotic solution for the viscoelastically modified solitary pressure pulse

In order to completely describe the evolution of the perturbed solitary pressure pulse it is important to correctly describe the dynamics of several subregions (see Fig. 1) ahead of, behind, and in the neighbourhood of the main pulse. In what follows it is convenient to discuss each subregion separately.

The perturbation field which is localized about the main pulse (that is, region 1; see Fig. 1) can be calculated using a straightforward comoving *adiabatic* asymptotic expansion. The solitary wave itself undergoes an algebraic decay in the amplitude and hence translation speed. There is also a monotonically increasing positive phase shift induced by the dissipation. The modulated amplitude, translation speed and phase shift are natural

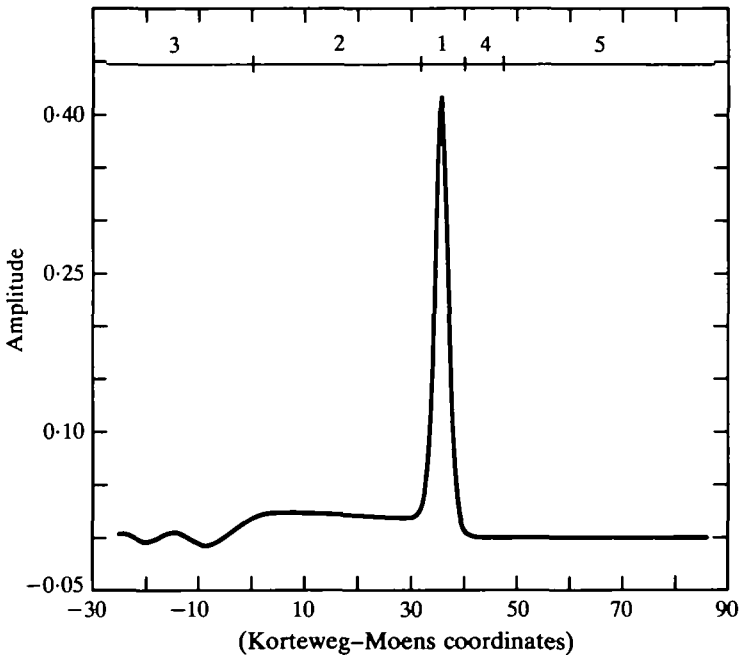


FIG. 1. The various solution regions required in order to correctly describe the viscoelastically modulated pressure pulse. In region 1 the $O(1)$ -amplitude main pulse and $O(\mu)$ -amplitude perturbation pressure can be obtained via an adiabatic expansion in comoving coordinates. Region 2 corresponds to the $O(\mu)$ -amplitude residual tube dilation excited by the passage of the perturbed soliton. Region 3 is the $O(\mu)$ -amplitude high-wavenumber wavetail which describes the transition back to a state of zero pressure. The transition from region 2 to region 3 occurs at the steadily-travelling Korteweg-Moens phase position. Region 4 corresponds to the near field *ahead* of the main pulse in which the exponentially-decaying leading-order pressure can be obtained via a combination WKB-power-series method. Region 5 corresponds to the far field *ahead* of the main pulse in which the exponentially-decaying leading-order pressure can be obtained via a combination WKB-similarity-solution method

consequences of the perturbed evolution of the scattering data in the inverse-scattering (IST) formulation (21, 23). Alternatively, it is possible to obtain the modulation in a direct singular perturbation theory as the consequence of the perturbed solitary wave attempting to satisfy leading- and secondary-order energy balances for the dissipative system (25, 40). Both these approaches are, of course, equivalent.

We shall show that ahead of the solitary pressure pulse the comoving adiabatic perturbation pressure for region 1 is algebraically non-uniform. (This property is similar to the non-uniformity found for KdV with Rayleigh damping (20, 25).) By modifying procedures developed by Johnson (20) we are able to construct a WKB approximation for the uniformly valid

leading-order pressure field in the near field (region 4, see Fig. 1) in which the phase and amplitude functions are obtained in the form of a power series in the Korteweg–Moens phase variable. In the far field ahead of the main pulse (region 5, see Fig. 1) we are able to obtain an exact similarity solution for the WKB phase and amplitude functions.

Behind the main pulse the adiabatic solution becomes exponentially non-uniform since a slowly-varying $O(\mu)$ -amplitude shelf (region 2 in Fig. 1) is being continuously excited by the propagating perturbed solitary wave. Physically, the shelf is excited because the modulated pressure pulse cannot simultaneously satisfy energy and mass-balance laws (41). From the point of view of the perturbed IST formalism (22, 23), the shelf emerges due to a zero-wavenumber resonance in the evolution of the scattering data. The transition from the shelf to the background null state is described by a similarity solution corresponding to the excitation of viscoelastically modified spatially-decaying $O(\mu)$ -amplitude dispersive waves (region 3, see Fig. 1) at a point in space or time corresponding to the Korteweg–Moens phase position (22, 23). Thus the action of the viscoelasticity on the solitary pressure pulse will be to excite a trailing small-amplitude wave train.

3.1 Adiabatic solution

3.1.1. *Evolution of the $O(1)$ pressure pulse.* In the absence of viscoelasticity (that is, $\mu = 0$), the soliton solution to (2.33a) is given by

$$q = -2\eta^2 \operatorname{sech}^2 [\eta(\theta - 4\eta^2\tau - \xi_0)], \tag{3.1}$$

where η and ξ_0 are arbitrary real parameters. The maximum absolute amplitude of the soliton is $2\eta^2$ and the propagation speed is $4\eta^2 > 0$. Thus the amplitude corrections included in (3.1) induce the pulse to travel at a higher speed than the Korteweg–Moens velocity. The parameter ξ_0 is a possible phase shift.

In the region where the soliton amplitude dominates the signal, an adiabatic multiple-scales perturbation solution to (2.33) can be constructed in the form

$$q \sim q^{(0)}(\xi; \chi) + \mu q^{(1)}(\xi; \chi) + \dots, \tag{3.2}$$

where ξ is a rapidly-varying soliton phase variable

$$\xi \equiv \theta - 4\mu^{-1} \int_0^{\mu\tau} \eta^2(\tau') d\tau', \tag{3.3a}$$

with derivatives given by

$$\xi_\theta = 1 \quad \text{and} \quad \xi_\tau = -4\eta^2(\chi), \tag{3.3b}$$

where χ is the stretched space variable given by

$$\chi = \mu\tau \equiv \frac{1}{16}\mu X(1 + 8\delta). \tag{3.3c}$$

In addition to allowing the propagation velocity to be a function of distance

travelled, we allow the phase shift to have a similar form; that is,

$$\xi_0 \equiv \xi_0(\chi). \tag{3.3d}$$

With no loss of generality we assume that at $x = 0$ the pulse is centred at $t = 0$ (that is, the signalling problem) so that

$$\xi_0(0) = 0. \tag{3.3e}$$

Substitution of (3.3) into (2.33) implies that

$$-4\eta^2 q_\xi - 6q q_\xi + q_{\xi\xi\xi} = \mu q_{\xi\xi} - \mu q_\chi. \tag{3.4}$$

The $O(1)$ problem for the expansion (3.2) is given by

$$-4\eta^2 q_\xi^{(0)} - 6q^{(0)} q_\xi^{(0)} + q_{\xi\xi\xi}^{(0)} = 0, \tag{3.5}$$

for which we take as the solution the soliton

$$q^{(0)} = -2\eta^2 \operatorname{sech}^2 [\eta(\xi - \xi_0)]. \tag{3.6}$$

The $O(\mu)$ problem can be put into the form

$$\mathcal{L}(q^{(1)}) = F_1(q^{(0)}), \tag{3.7a}$$

where

$$\mathcal{L}(q^{(1)}) \equiv -4\eta^2 q_\xi^{(1)} - 6(q^{(1)} q^{(0)})_\xi + q_{\xi\xi\xi}^{(1)}, \tag{3.7b}$$

$$F_1(q^{(0)}) \equiv q_{\xi\xi}^{(0)} - q_\chi^{(0)} \tag{3.7c}$$

$$= q_{\xi\xi}^{(0)} - \frac{1}{\eta} \eta_\chi \{2q^{(0)} + (\xi - \xi_0) q_\xi^{(0)}\} + \xi_{0\chi} q_\xi^{(0)}. \tag{3.7d}$$

We shall construct an exact solution to (3.7a) in the next subsection. Here, we focus on determining the evolution of $\eta(\chi)$ and $\xi_0(\chi)$.

The dependence of η and ξ_0 on the stretched coordinate χ can be obtained as solvability conditions for the perturbation expansion (3.2) (25, 42), as a result of averaged conservation laws (40), or directly from the evolution of the scattering data in the perturbed IST formalism (21, 23). Again, all these approaches are, of course, equivalent.

The evolution of η can be obtained as a solvability condition on (3.7a) by noting that $q^{(0)}(\xi; \chi)$ is an element of the kernel of the homogeneous adjoint operator associated with \mathcal{L} in (3.7). (Note that the adjoint to \mathcal{L} is simply the negative of the KdV operator.) Thus $q^{(0)}(\xi; \chi)$ must be orthogonal to $F_1(q^{(0)})$; that is,

$$\frac{1}{2} \partial_\chi \int_{-\infty}^{\infty} q^{(0)2} d\xi = \int_{-\infty}^{\infty} q^{(0)} q_{\xi\xi}^{(0)} d\xi, \tag{3.8}$$

which is the leading-order phase-averaged energy balance for (2.33). Direct calculation of (3.8) yields the relation

$$\eta_\chi = -\frac{1}{138} \eta^3, \tag{3.9}$$

for which the general solution is

$$\eta(\chi) \equiv [15\eta^2(0)/(16\eta^2(0)\chi + 15)]^{1/2} \tag{3.10}$$

(see Fig. 2a), where $\eta(0)$ is the initial condition on $\eta(\chi)$.

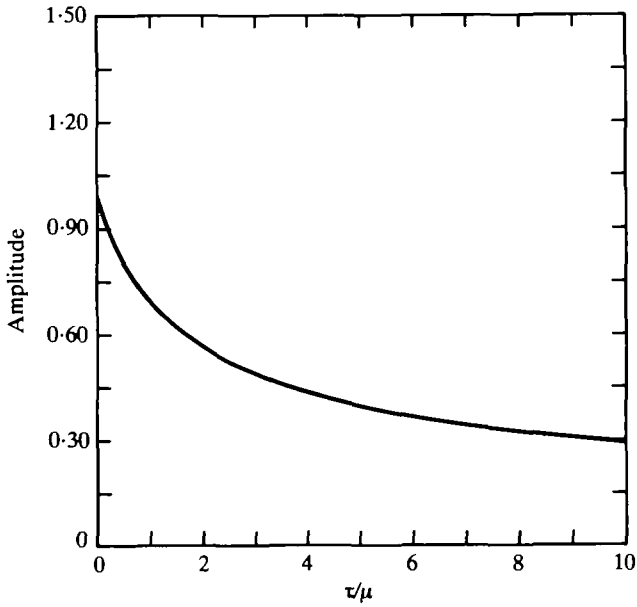


FIG. 2a. The viscoelastically-induced evolution of the soliton amplitude parameter $\eta(\chi)$ as a function of the stretched spatial coordinate $\chi = \mu\tau$ assuming that $\eta(0) = 1$

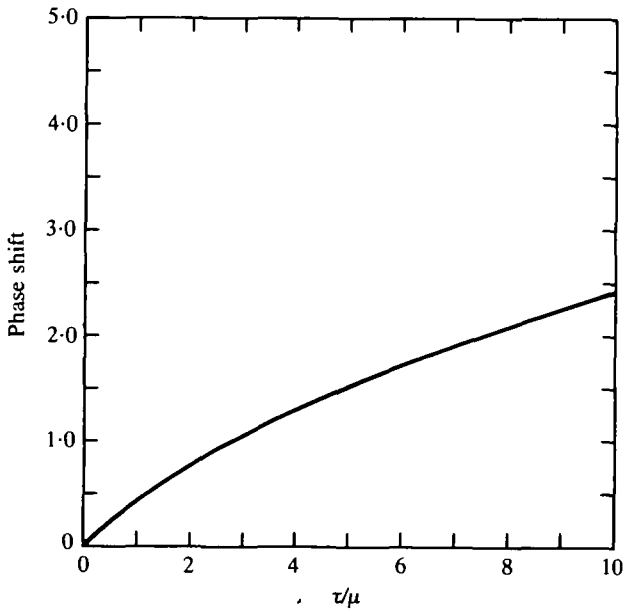


FIG. 2b. The viscoelastically-induced evolution of the $O(\mu)$ phase shift $\xi_0(\chi)$ assuming that $\eta(0) = 1$

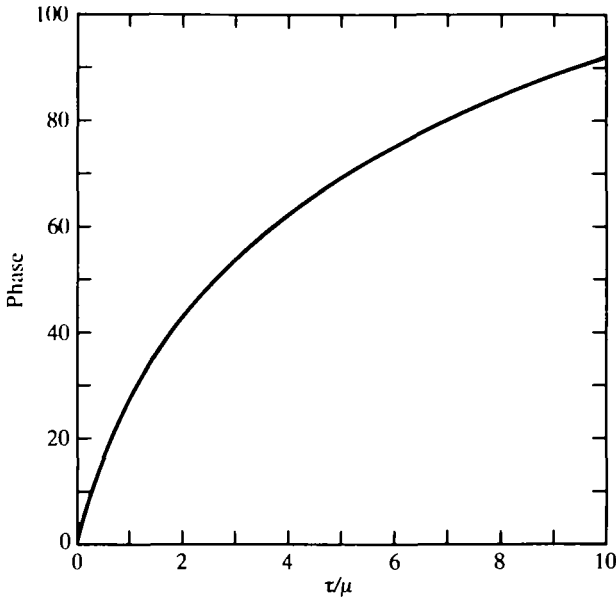


FIG. 2c. The viscoelastically modulated soliton phase position $\theta_e(\chi)$ relative to the Korteweg–Moens phase $\theta = 0$ assuming that $\eta(0) = 1$

The derivation of the ordinary differential equation determining $\xi_0(\chi)$ is much more delicate to obtain but, physically, can be most simply viewed as the result of higher-order energy balances (42). However, the spatial dependence of $\xi_0(\chi)$ as determined by the IST formalism (22, equation (2.46)) is easy to state:

$$\xi_{0\chi} = -(4\eta^3)^{-1} \int_{-\infty}^{\infty} q_{\xi\xi}^{(0)}(\xi; \chi) \{ \xi \operatorname{sech}^2(\xi) + \tanh(\xi) + \tanh^2(\xi) \} d\xi. \quad (3.11)$$

Calculation of the right-hand side of (3.11) implies that

$$\xi_{0\chi} = 8\eta/15, \quad (3.12)$$

which can be solved subject to (3.3e) to give

$$\xi_0(\chi) = [1 + 16\eta^2(0)\chi/15]^{1/2} / \eta(0) - 1/\eta(0). \quad (3.13)$$

In contrast to the exponential decay of the amplitude and exponential growth in the phase shift for the KdV soliton when modulated by Rayleigh damping (23), the viscoelastically induced decay in the amplitude and growth in the phase shift found here is algebraic. On heuristic grounds this result is not surprising, since (2.33) without nonlinearity and dispersion is simply the 1 + 1 heat equation.

3.1.2. *The adiabatic perturbation pressure field.* With the structure of $\eta(\chi)$

and $\xi_0(\chi)$ determined, the leading-order behaviour of the dissipating solitary wave is complete. We turn now to obtaining a closed-form solution for the comoving perturbation pressure $q^{(1)}(\xi; \chi)$.

We begin by noting that (3.7) can be integrated once immediately to give the second-order differential equation

$$\begin{aligned} & \{\partial_{\xi\xi}^2 + 12\eta^2 \operatorname{sech}^2[\eta(\xi - \xi_0)] - 4\eta^2\}q^{(1)} \\ & = 44\eta^3 \tanh[\eta(\xi - \xi_0)]/15 - 16\eta^4(\xi - \xi_0) \operatorname{sech}^2[\eta(\xi - \xi_0)]/15 \\ & \quad - 2\eta^2\xi_{0\chi} \operatorname{sech}^2[\eta(\xi - \xi_0)] - 4\eta^3 \tanh^3[\eta(\xi - \xi_0)] + \Gamma(\chi), \end{aligned} \quad (3.14)$$

where $\Gamma(\chi)$ is a constant of integration. If we impose the condition that ahead of the solitary wave the tube remains undisturbed (that is, $q^{(1)} \rightarrow 0$ as $\xi \rightarrow +\infty$), it follows from (3.14) that

$$\Gamma(\chi) = 16\eta^3(\chi)/15. \quad (3.15)$$

Consequently, it follows from (3.14) that

$$q^{(1)}(\xi; \chi) \rightarrow -8\eta(\chi)/15 \quad (3.16)$$

as $\xi \rightarrow -\infty$. Hence there is an algebraically decaying shelf created behind the dissipating solitary wave (see region 2 in Fig. 1). The shelf is created because the adiabatically modulated soliton cannot simultaneously satisfy mass *and* energy-balance laws. The creation of the shelf region for the perturbed KdV was predicted analytically by Johnson (20) and Leibovich and Randall (43), among others, and numerically observed by the latter authors as well. The prediction of the emergence of a shelf arises quite naturally in the IST formalism for the perturbed KdV equation (23).

The fact that (3.16) holds implies that the expansion (3.2) is exponentially non-uniform as $\xi \rightarrow -\infty$. In sections 3.2 and 3.3 the direct asymptotic procedures of Knickerbocker and Newell (24) and Smyth (26) are modified to determine the transition about $\theta = 0$ of the shelf back to a zero background state and the subsequent evolution of the shelf region after its initial formation.

With $\Gamma(\chi)$ given by (3.15) it is now possible to solve (3.14) explicitly for $q^{(1)}(\xi; \chi)$. Following Kodama and Ablowitz (25) we introduce the new independent variable

$$\zeta \equiv \tanh[\eta(\xi - \xi_0)] \quad (3.17)$$

into (3.14). It follows that (3.14) can be rewritten in the form

$$\begin{aligned} & \{(1 - \zeta^2)q_{\zeta\zeta}^{(1)}\}_{\zeta} + [12 - 4(1 - \zeta^2)^{-1}]q^{(1)} \\ & = (4\zeta^2 + 4\zeta + \frac{16}{15})(1 + \zeta)^{-1}\eta - 2\xi_{0\chi} - 8\eta \ln [(1 + \zeta)/(1 - \zeta)]/15. \end{aligned} \quad (3.18)$$

Equation (3.18) is an inhomogeneous associated Legendre equation (44) for which the homogeneous regular solution is given by $q^{(1)} = P_3^2(\zeta) \equiv 15\zeta(1 - \zeta^2)$. The particular solution can be constructed by the

method of variation of parameters; that is,

$$q^{(1)} = \Phi(\xi)P_3^2(\xi). \quad (3.19)$$

Substitution of (3.19) into (3.18) leads to

$$\begin{aligned} [\xi^2(1-\xi^2)^3\Phi_\xi]_\xi = & \frac{(16\xi + 44\xi^2 - 60\xi^4)\eta}{225} - \frac{2\xi(1-\xi^2)\xi_{0x}}{15} \\ & - \frac{8\eta\xi(1-\xi^2)\ln[(1+\xi)/(1-\xi)]}{225}. \end{aligned} \quad (3.20)$$

This equation can easily be integrated twice immediately to imply that $q^{(1)}$ is given by

$$\begin{aligned} q^{(1)}(\xi; \chi) = & 4\eta[\tanh(\phi) - 1]/15 + (4\eta/4 - 15\xi_{0x}) \operatorname{sech}^2(\phi) \times \\ & \times [\phi \tanh(\phi) - 1] + 2\eta\phi \operatorname{sech}^2(\phi)[\phi \tanh(\phi) - 2], \end{aligned} \quad (3.21)$$

where for convenience we define $\phi \equiv \eta(\xi - \xi_0)$.

Note that as $\xi \rightarrow +\infty$ (3.21) implies that

$$q^{(1)} \sim 8\eta\phi^2 \exp(-2\phi)/15, \quad (3.22a)$$

whereas as $\xi \rightarrow -\infty$ (3.21) implies that

$$q^{(1)} \sim -8\eta[1 + \phi^2 \exp(2\phi)]/15. \quad (3.22b)$$

It follows from (3.22a) that the expansion (3.2) is algebraically non-uniform ahead of the propagating pressure pulse. In section 3.4 we shall remove this non-uniformity by the introduction a WKB-power-series and similarity-solution procedure.

3.2 Shelf emergence and subsequent evolution

The perturbation pressure field given by (3.21) predicts the creation of a shelf region behind the main portion of the propagating pulse with slowly-varying amplitude described by (3.16). However, (3.16) only describes the initial formation of the shelf immediately behind the solitary pressure pulse and not the subsequent evolution of the entire shelf tail. In this section we shall describe the subsequent evolution of the shelf.

We are assuming that at $x = 0$ the solitary pulse is centred at $t = 0$. Hence for $\tau \geq 0$ the leading-order phase position relative to the Korteweg-Moens phase (that is, $\theta = 0$) of the solitary pressure pulse is given by

$$\theta_c(\chi) \equiv \frac{4}{\mu} \int_0^\chi \eta^2(\chi') d\chi', \quad (3.23a)$$

which on account of (3.10) can be put into the form

$$\theta_c(\chi) \equiv 15(4\mu)^{-1} \ln [1 + 16\eta^2(0)\chi/15] \quad (3.23b)$$

(see Fig. 2c).

In the region $0 < \theta < \theta_c(\chi)$ the amplitude of the shelf is small (that is, $O(\mu)$) and varies slowly with respect to the variables τ and θ (that is, the τ and θ derivatives are $O(\mu)$) (24, 25, 26). Thus, in this slowly-varying small-amplitude shelf region the evolution of the tail will be described by an asymptotic expansion of the form

$$q \sim \mu \hat{q}^{(0)}(\chi, \Theta) + \mu^2 \hat{q}^{(1)}(\chi, \Theta) + \dots, \quad (3.24a)$$

where χ is the stretched-space variable given in (3.3c) and Θ is a stretched Korteweg–Moens phase variable given by $\Theta = \mu\theta$.

Substitution of the expansion (3.24a) into (2.33) will imply that the leading-order dynamics of this region of the shelf tail will be described by

$$\hat{q}_\chi^{(0)} = 0, \quad (3.24b)$$

with the moving boundary conditions

$$\hat{q}^{(0)}(\chi, \Theta = \mu\theta_c(\chi)) = -8\eta(\chi)/15. \quad (3.24c)$$

The boundary condition (3.24c) expresses the requirement that the magnitude of the newly created shelf following the dissipating soliton is determined by the asymptotic behaviour of $q^{(1)}(\xi, \chi)$ for $\xi \rightarrow -\infty$ as determined by (3.16). The solution to (3.24) is straightforward to obtain and implies that the leading-order evolution of the shelf can be written in the form

$$q(\chi, \theta) \sim -8\mu\eta[\hat{\chi}(\theta)]/15, \quad (3.25a)$$

where $\hat{\chi}(\theta)$ is given by

$$\hat{\chi}(\theta) = \begin{cases} 15[\exp(4\mu\theta/15) - 1]/[16\eta^2(0)] & \text{for } 0 < \theta < \theta_c, \\ 0 & \text{elsewhere.} \end{cases} \quad (3.25b)$$

3.3 Formation and evolution of the dispersive wavetail

The solution obtained for the evolution of the shelf-tail region does not correctly describe the transition back to a zero background pressure field in $\theta < 0$ which begins in the neighbourhood of $\theta = 0$. This transition is dominated by $O(\mu)$ -amplitude high-wavenumber spatially-decaying oscillations (that is, a dispersive wavetail) (24, 26). Mathematically, the evolution of the dispersive wavetail is assumed to be described by an asymptotic expansion of the form

$$q \sim \mu \bar{q}^{(0)}(\tau, \theta) + \mu^2 \bar{q}^{(1)}(\tau, \theta) + \dots \quad (3.26a)$$

Substitution of (3.26a) into (2.33) will imply that the leading-order dynamics of the dispersive wavetail will be described by

$$\bar{q}_\tau^{(0)} + \bar{q}_{\theta\theta\theta}^{(0)} = 0, \tag{3.26b}$$

with the boundary conditions

$$\bar{q}^{(0)}(\tau, \theta) \rightarrow \begin{cases} 0 & \text{as } \theta \rightarrow -\infty, \\ -8\eta(0)/15 & \text{as } \theta \rightarrow +\infty, \end{cases} \tag{3.26c}$$

for all $\tau > 0$, where (3.26c) represents the leading-order term of the shelf-tail solution (3.25a) near the Korteweg–Moens phase position $\theta = 0$. The solution to (3.26) implies that the leading-order formation and evolution of the dispersive wavetail will be described by

$$q(\tau, \theta) \sim -\{\mu 8\eta(0)/15\} \int_{-\infty}^{\theta(3\tau)^{-1/3}} \text{Ai}(s) ds, \tag{3.27}$$

where $\text{Ai}(s)$ is the bounded Airy function.

3.4 Structure of the pressure field ahead of the propagating main pulse

We showed in section 3.1.2 that the adiabatic perturbation field is algebraically non-uniform in the soliton phase variable ξ as $\xi \rightarrow +\infty$. In this section we construct a uniformly valid representation of the perturbation field ahead of the solitary pressure pulse via a combination WKB–power-series similarity-solution procedure. The methods exploited in this section are modifications of the methods developed by Johnson (20) and Kodama and Ablowitz (25) for the KdV equation perturbed with Rayleigh damping.

When the phase variable satisfies $0 \ll (\xi - \xi_0) \sim O(\mu^{-1})$, an asymptotic solution to (2.33) can be obtained in the form

$$q \approx q^\dagger(Z, \chi), \tag{3.28a}$$

where Z is a stretched soliton phase variable given by

$$Z \equiv \mu \left\{ \theta - \frac{4}{\mu} \int_0^x \eta^2(\tau') d\tau' - \xi_0(\chi) \right\}. \tag{3.28b}$$

Substitution of (3.28) into (2.33a) implies that $q^\dagger(Z, \chi)$ is approximately governed by

$$q_x^\dagger - 4\eta^2(\chi)q_z^\dagger = \mu^2 q_{zz}^\dagger - \mu^2 q_{zzz}^\dagger. \tag{3.29}$$

In writing (3.29) we have neglected the nonlinear terms for the following reason. The solution of (3.29) will have to match the leading-order behaviour of the soliton plus perturbation pressure field in the limit as $\xi \gg 1$. However, it follows from (3.6) and (3.22a) that $q^{(0)} + \mu q^{(1)}$ will be exponentially decaying in this region. Therefore the quadratic nonlinear term in (2.33a) will be exponentially small in comparison with the terms in (3.29) and can consequently be omitted in our leading-order analysis.

The required matching condition on the solution to (3.29) is that

$$q^\dagger(Z, \chi) \rightarrow 8\eta^2(\chi)[-1 + \eta(\chi)(15\mu)^{-1}Z^2] \exp[-2\eta(\chi)Z/\mu] \quad (3.30)$$

as $Z \rightarrow 0$. The right-hand side of (3.20) is simply $q^{(0)}(\xi, \chi) + \mu q^{(1)}(\xi, \chi)$, with $q^{(0)}$ and $q^{(1)}$ given by (3.6) and (3.21), respectively, for $\xi - \xi_0 \gg 0$ in terms of the stretched phase variable (3.28b). In addition, we also require the solution to (3.29) to vanish exponentially rapidly as $Z \rightarrow +\infty$.

The algebraic non-uniformities can be eliminated by constructing a leading-order WKB solution (Bender and Orszag (45)) for (3.29) in the form

$$q^\dagger \sim h(Z, \chi) \exp\left[\frac{1}{\mu}f(Z, \chi)\right] + O(\mu). \quad (3.31a)$$

Substitution of (3.31a) into (3.29) results in the pair of equations

$$\left. \begin{aligned} f_\chi - 4\eta^2(\chi)f_z + (f_z)^3 &= 0, \\ h_\chi - 4\eta^2(\chi)h_z + 3\{hf_z f_{zz} + h_z(f_z)^2\} &= h(f_z)^2. \end{aligned} \right\} \quad (3.31b)$$

3.4.1. The near-field WKB power-series solution

When Z is small (for example, in the near-field region) the matching condition (3.30) suggests a power-series solution in the form

$$\left. \begin{aligned} f(Z, \chi) &= \alpha_1(\chi)Z + \alpha_2(\chi)Z^2 + \dots, \\ h(Z, \chi) &= \beta_0(\chi) + \beta_1(\chi)Z + \dots \end{aligned} \right\} \quad (3.32)$$

Substitution of (3.32)₁ into (3.31b)₁ implies that

$$\left. \begin{aligned} \alpha_1(\chi) &= -2\eta(\chi), \\ \alpha_2(\chi) &= \alpha_{1z} [8\eta^2 - 6(\alpha_1)^2]^{-1} = -\eta(\chi)/15, \end{aligned} \right\} \quad (3.33)$$

and so on for the expansion coefficients for the phase function $f(Z, \chi)$.

From the WKB amplitude equation (3.31b)₂ we find that $\beta_0(\chi)$ is undetermined and that

$$\beta_1(\chi) = \{\beta_{0z} + 6\beta_0\alpha_1\alpha_2 - \beta_0(\alpha_1)^2\} \{4\eta^2 - 3(\alpha_1)^2\}^{-1}. \quad (3.34)$$

However, the asymptotic matching condition (3.30) requires that

$$\beta_0(\chi) = -8\eta^2(\chi). \quad (3.35a)$$

Substitution of (3.35a) into (3.34) implies that

$$\beta_1(\chi) = -64\eta^2(\chi)/15. \quad (3.35b)$$

Hence the leading-order near-field representation for $q^\dagger(Z, \chi)$ can be put into the form

$$q^\dagger(Z, \chi) \sim -8\eta^2(\chi)[1 + 8Z/15] \exp\{-2\eta(\chi)[1 + Z/30]Z/\mu\}. \quad (3.36)$$

Note that, as $Z \rightarrow 0$, (3.36) will imply that

$$q^\dagger(Z, \chi) \sim 8\eta^2[-1 + \eta Z^2/15\mu] \exp[-2\eta Z/\mu],$$

which exactly matches (3.30), including the $O(\mu^{-1})$ term.

3.4.2. *The far-field WKB similarity solution.* As $Z \rightarrow +\infty$ the power-series solution (3.32) is no longer valid and a similarity solution for the WKB equations (3.31) is required. The exact similarity solution to (3.31) is most conveniently expressed in the stretched Korteweg-Moens phase variable

$$\Theta \equiv Z + 4 \int_0^x \eta^2(\tau') d\tau' \equiv \mu\theta. \tag{3.37}$$

Substitution of (3.37) into (3.31) yields

$$\left. \begin{aligned} f_\chi + (f_\Theta)^3 &= 0, \\ h_\chi + 3\{hf_\Theta f_{\Theta\Theta} + h_\Theta(f_\Theta)^2\} &= h(f_\Theta)^2. \end{aligned} \right\} \tag{3.38}$$

The phase equation (3.38)₁ has the exact similarity solution

$$f(\chi, \Theta) \equiv -2(\Theta/3)^{\frac{1}{3}}\chi^{-\frac{1}{3}}, \tag{3.39}$$

which is just the exponent of the exponential approximation to the Airy function. Substitution of (3.39) in (3.38)₂ gives

$$\chi h_\chi + \Theta h_\Theta = \frac{1}{6}(2\Theta - 3)h. \tag{3.40}$$

It follows from (3.30), (3.31a), (3.37) and (3.39) that the appropriate matching condition can be written in the form

$$h(\chi, \Theta) \rightarrow -8\eta^2(\chi) \quad \text{as } \Theta \rightarrow \mu\theta_c(\chi). \tag{3.41}$$

The exact solution of (3.40) subject to (3.41) is

$$h(\chi, \Theta) = -8\eta^2(\bar{\chi})[\mu\theta_c(\bar{\chi})/\Theta]^{\frac{1}{3}} \exp\{\frac{1}{3}[\Theta - \mu\theta_c(\bar{\chi})]\}, \tag{3.42a}$$

where $\bar{\chi}$ is obtained from the relation

$$\Theta\bar{\chi} = \chi\mu\theta_c(\bar{\chi}). \tag{3.42b}$$

The solution (3.42) completes the leading-order asymptotic solution of the perturbation pressure field ahead of the main pulse.

4. Discussion

Figure 3 depicts the evolution of the soliton and complete perturbation-pressure field under the action of weak viscoelasticity. The solution as drawn is a uniformly valid asymptotic representation for $q(\tau, \theta)$ obtained, in the usual way (45), by adding together the asymptotic representations for the individual regions (see Fig. 1) as derived in section 3, and then subtracting the appropriate contributions in the overlap zones between the

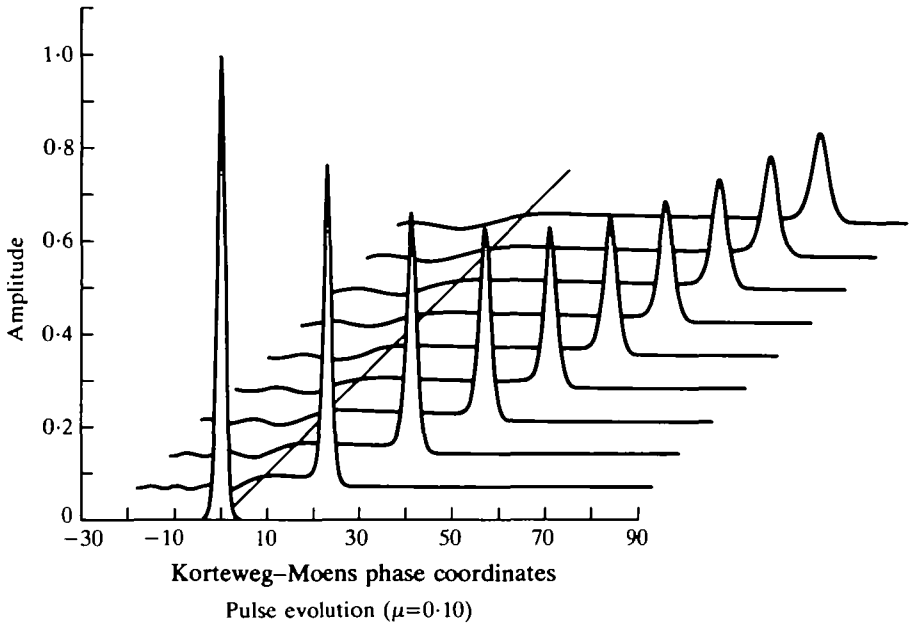


FIG. 3. A Korteweg-Moens phase-space plot of the normalized uniformly valid soliton plus perturbation-pressure field $-[q^{(0)} + \mu q^{(1)}]/[2\eta^2(0)]$ for τ values of 0, 5, 10, ..., 45, respectively. The τ -axis which is oriented into the page corresponds to the phase position of the Korteweg-Moens phase (that is, $\theta = 0$)

regions. The horizontal axis corresponds to the phase coordinate of the soliton relative to the Korteweg-Moens phase which is the straight line in Fig. 3 (recall that the Korteweg-Moens phase corresponds to the non-dimensional physical variable given by $\theta \equiv x - t$). The pulses shown correspond to a sequence $\tau = \{0, 5, \dots, 45\}$; recall that $\tau = \frac{1}{16}\epsilon x(1 + 8\delta)$. Throughout this section $\mu = 0.1$.

Figure 3 illustrates the relatively slow algebraic decay in the soliton amplitude and concomitant broadening in the pulse shape (due to the presence of $\eta(x)$ multiplying the entire phase in (3.6)). Note that Fig. 3 also illustrates the stretching of the oscillation wavelength in the dispersive wavetail due to the combined effects of the form of the similarity variable in (3.27) and viscoelastic dissipation.

Figure 4 depicts the uniformly valid (obtained as described above) pulse evolution as a function of non-dimensional time for a sequence of non-dimensional stations (distance in tube radii ahead of the region of soliton excitation) given by 0, 10, 20, ..., 90 tube radii. Here, the straight line in Fig. 4 corresponds to the point of excitation (that is, no tube radii). Very little viscoelastic amplitude decay is shown because of the relatively short

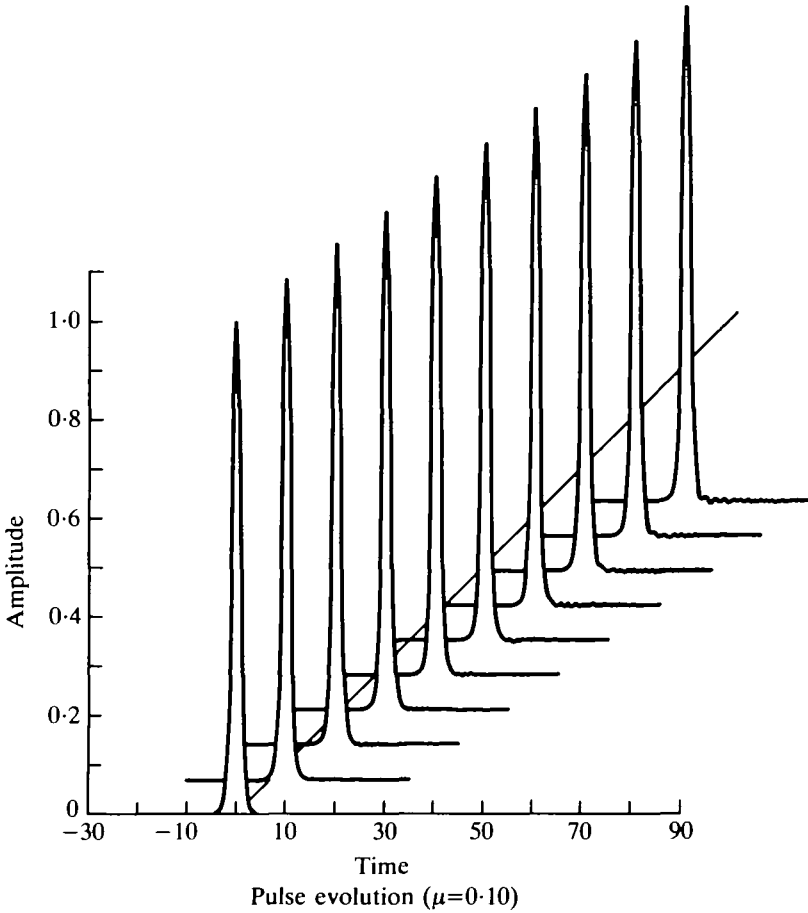


FIG. 4. A space-time plot of the normalized uniformly valid solitary pressure pulse plus perturbation pressure field $-[q^{(0)} + \mu q^{(1)}]/[2\eta^2(0)]$ as a function of distance travelled down-tube in tube radii. The horizontal axis corresponds to non-dimensional time and the sequence of sections shown corresponds to stations located at 0, 10, 20, ..., 90 tube radii, respectively

distance travelled (recall that one tube radius is $\epsilon^{1/2} \sim 0.1$ soliton-length units). Figure 4 illustrates the early formation of the pressure shelf and dispersive wavetail. Both the soliton and wavetail travel down the tube but the soliton, because of nonlinearity, will move faster than the Korteweg-Moens phase speed, the speed at which the transition point from shelf to wavetail travels. It is also possible to see the very early formation and subsequent lengthening of the shelf region extending from behind the main pulse to the location of the Korteweg-Moens phase.

Figures 5a, b and c provide a detailed view of the uniformly valid

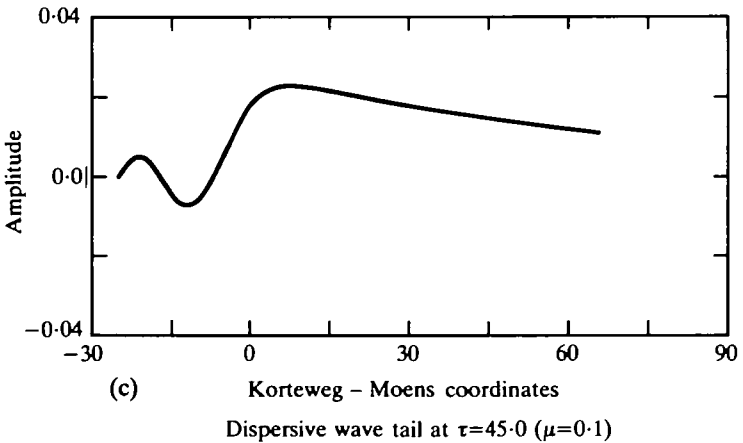
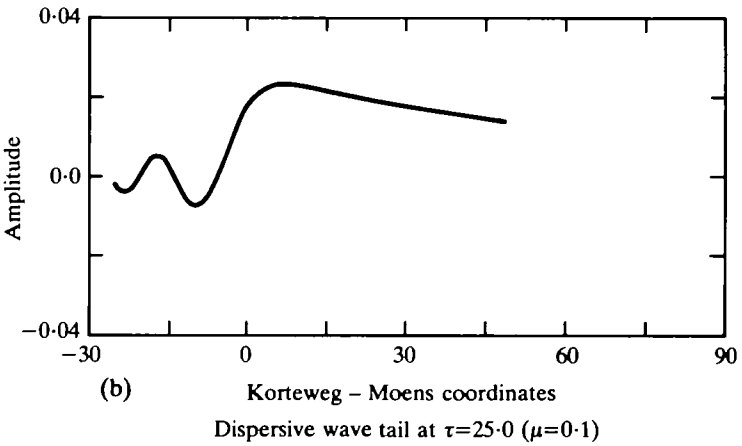
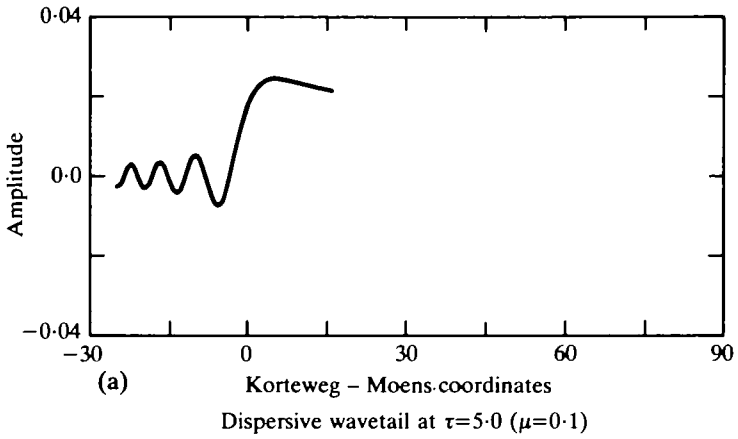


FIG. 5. Sequence of figures illustrating the formation and evolution of the normalized uniformly valid shelf and dispersive wavetail given by $[(3.25a) + (3.27) - (3.26c)_2]/[-2\eta^2(0)]$. Figures 5a, b and c correspond to $\tau = 5, 25$ and 45 , respectively

(obtained as described above) evolution of the shelf and dispersive wavetail at $\tau = 5.0, 25.0$ and 45.0 , respectively.

5. Summary and conclusions

A direct singular-perturbation theory has been developed to describe the viscoelastic modulation of solitary pressure pulses in a nonlinear fluid-filled tube for small retardation times. We have shown that the propagation of these solitary pulses is governed by a Korteweg–de Vries–Burgers equation. The action of the viscoelasticity results in an algebraically decaying amplitude and translation speed of the pulse (with the limit being the classical Korteweg–Moens phase speed of the linear hyperbolic theory). As well, a monotonically increasing positive phase shift is induced that is of the order of the non-dimensional characteristic time. Behind the main pulse a pressure shelf of finite extent is continuously created corresponding to a residual dilation of the tube. The shelf extends from the main pulse to the position corresponding to the location of a Korteweg–Moens phase. The transition of the pressure shelf to a zero background state occurs at the location of the Korteweg–Moens phase in the form of viscoelastically modified spatially-decaying high-wavenumber oscillations.

A complete description of the perturbed field ahead of the main pulse was also given. Near the main pulse the leading-order pressure field can be obtained in the form of a WKB solution in which the phase and amplitude functions can be obtained as a power series in a stretched soliton phase variable. Further ahead of the main pulse, the power-series solution is no longer valid but an exact similarity solution can be obtained. Finally, an exact solution for the perturbation pressure comoving with the modulated soliton can be derived via the adiabatic ansatz.

Unfortunately, the available experimentally obtained time-series data of pressure pulses travelling in a viscoelastic tube (for example, (8, 9, 11, 12)) are of insufficient quality to be able to directly test the predictions of the fairly subtle asymptotic balances we have examined in this paper. However, we can make some simple suggestions concerning possible experimental work with this aim in mind. One of the most striking predictions of our calculations is the formation, subsequent lengthening and eventual dissipation of the *shelf* region which separates the dispersive wavetail and main pulse. It would be very interesting to attempt to observe and measure this process.

Another line of possible future analytical or computational research is to generalize the special soliton initial condition we have assumed to more arbitrary initial conditions. The present authors have undertaken a numerical study of (2.33) with this aim in mind and will report on this work in a future paper.

Acknowledgements

The authors would like to thank Professor T. Bryant Moodie for many helpful discussions on this research and for commenting on a first draft on this paper. The authors would also like to thank Professors Robert J. Tait and Robert F. Millar for many helpful discussions. The research of the first author is supported by Operating Research Grants from the Natural Sciences and Engineering Research Council of Canada. The research of the second author is supported by a Post-doctoral Fellowship awarded by the Natural Sciences and Engineering Research Council of Canada.

REFERENCES

1. M. J. LIGHTHILL, *Waves in Fluids* (University Press, Cambridge 1978).
2. H. W. MICHOLSON, W. H. HEISER and J. H. OLSEN, *Bull. Mech. Engrg Educ.* **6** (1967) 371–376.
3. G. RUDINGER, *Proceedings, Biomedical Fluid Mechanics Symposium* (1966) 1–33.
4. S. J. COWLEY, *J. Fluid Mech.* **116** (1982) 459–473.
5. —, *Q. Jl Mech. appl. Math.* **36** (1983) 284–312.
6. A. E. GREEN and W. ZERNA, *Theoretical Elasticity*, 2nd edition (Oxford University Press, London 1968).
7. C. G. CARO, T. J. PEDLEY, R. C. SCHROTER and W. A. SEED *The Mechanics of the Circulation* (University Press, Oxford 1978).
8. S. E. GREENWALD and D. L. NEWMAN, *Med. Biol. Engrg Comput.* **20** (1982) 697–701.
9. D. L. NEWMAN, S. E. GREENWALD and T. B. MOODIE, *Med. Biol. Engrg Comput.* **21** (1983) 697–701.
10. T. B. MOODIE, F. MAINARDI and R. J. TAIT, *Meccanica* **20** (1985) 33–37.
11. —, D. W. BARCLAY, S. E. GREENWALD and D. L. NEWMAN, *Acta Mech.* **54** (1984) 107–119.
12. —, — and —, *ibid.* **59** (1986) 47–58.
13. T. J. PEDLEY, *The Fluid Mechanics of Large Blood Vessels* (University Press, Cambridge 1980).
14. I. KECECIOGLU, M. E. MCCLURKEN, R. D. KAMM and A. H. SHAPIRO, *J. Fluid Mech.* **109** (1981) 367–389.
15. T. B. MOODIE and J. B. HADDOW, *Int. J. Nonlinear Mech.* **12** (1977) 223–231.
16. M. E. MCCLURKEN, I. KECECIOGLU, R. D. KAMM and A. H. SHAPIRO, *J. Fluid Mech.* **109** (1981) 391–415.
17. G. E. SWATERS, *Z. angew. Math. Phys.* **39** (1988) 668–681.
18. S. J. COWLEY, Ph.D. Dissertation, University of Cambridge (1981).
19. R. RAVINDRAN and P. PRASAD, *Acta Mech.* **31** (1979) 253–280.
20. R. S. JOHNSON, *J. Fluid Mech.* **60** (1973) 813–824.
21. V. I. KARPMAN, *Phys. Lett. A* **60** (1977) 307–308.
22. — and E. M. MASLOV, *Sov. Phys. JETP* **48** (1978) 252–259.
23. D. J. KAUP and A. C. NEWELL, *Proc. R. Soc. A* **361** (1978) 413–446.
24. C. J. KNICKERBOCKER and A. C. NEWELL, *J. Fluid Mech.* **98** (1980) 803–818.
25. Y. KODAMA and M. J. ABLOWITZ, *Stud. appl. Math.* **64** (1981) 225–245.
26. N. F. SMYTH, Ph.D. Dissertation, California Institute of Technology (1984).
27. T. B. MOODIE, R. J. TAIT and J. B. HADDOW, In *Wave Propagation in Viscoelastic Media*, Research Notes in Mathematics **52** (ed. F. Mainardi; Pitman, London 1982) 124–168.

28. A. C. PIPKIN, *Lectures on Viscoelasticity Theory* (Springer, New York 1972).
29. R. P. SAWATZKY and T. B. MOODIE, *Q. Jl Mech. appl. Math.* **41** (1988) 33–50.
30. H. GRAD and P. N. HU, *Phys. Fluids* **10** (1967) 2596–2602.
31. B. I. COHEN, J. A. KROMMES, W. M. TANG and M. N. ROSENBLUTH, *Nucl. Fusion* **16** (1976) 971–992.
32. G. I. SIVASHINSKY, *Ann. Rev. Fluid Mech.* **15** (1983) 179–199.
33. T. KAWAHARA, *Phys. Rev. Lett.* **51** (1983) 381–383.
34. R. S. JOHNSON, *J. Fluid Mech.* **42** (1970) 49–60.
35. A. P. HOOPER and R. H. J. GRIMSHAW, *Phys. Fluids* **28** (1985) 37–45.
36. A. D. D. CRAIK, *Wave Interactions and Fluid Flows* (University Press, Cambridge 1985).
37. A. JEFFREY and T. KAKUTANI, *SIAM Rev.* **14** (1972) 582–643.
38. T. KAWAHARA and S. TOH, *Phys. Fluids* **28** (1985) 1636–1638.
39. B. A. MALOMED, *Physica* **29D** (1987) 155–172.
40. R. H. J. GRIMSHAW, *Proc. R. Soc. A* **368** (1979) 359–375.
41. A. C. NEWELL, *Solitons in Mathematics and Physics*, CBMS-NSF **48** (SIAM, Philadelphia 1985).
42. M. J. ABLOWITZ and H. SEGUR, *Solitons and the Inverse Scattering Transform* (SIAM, Philadelphia 1981).
43. S. LEIBOVICH and J. D. RANDALL, *J. Fluid Mech.* **58** (1973) 481–493.
44. G. ARFKEN, *Mathematical Methods for Physicists* (Academic Press, New York 1973).
45. C. M. BENDER and S. A. ORSZAG, *Advanced Mathematical Methods for Scientists and Engineers* (McGraw-Hill, New York 1978).